CHAPTER II
LITERATURE SURVEY AND ION-EXCHANGE KINETICS

2.1 Literature Survey

Erickson and Rase (1979) studied fixed bed ion exchange with different ionic mobilities and nonlinear equilibria. The preliminary model developed by Erickson and Rase employing fundamentally based parameters is proposed and tested against experimental data from the fixed bed column. The system selected for their study consisted of Dowex50-X8. Equilibrium relationships, ionic diffusion coefficients in the resin, dispersion coefficients, boundary layer, the film thicknesses, total exchange capacity, bed void fraction, and particle dimensions were determined experimentally. These data were then used in the model, which gave good agreement with the observed breakthrough curves.

Lin and Wu (1996) studied the removal of ammonia from aqueous solution by a strongly acid resin. They found that operating variables such as pH, initial ammonia concentration and temperature have a strong influence on the rate of exchange. Various ion exchange isotherms, including those of Langmuir, Freundlich, modified Langmuir and Jossens, were employed to correlate the experimental isotherm data. A mass transfer model based on the squared driving force was adopted and found to fit well with the experimental rate. The results indicated that the initial pH of the aqueous solution is highly critical for the ammonia removal. For efficient ion exchange removal of ammonia, the pH needs to be kept at or below 7.

Manantapong (1997) studied the behavior of exchanging of Na^+ ions on the strong-acid cation resin (Dowex50-X8), which was placed in a packed column. This column work was operated in upflow as a fluidized bed. The study of adsorption kinetics was first carried out with batch operation, so that

the concept of degree of relative volatility was suitable for describing the experimental data. The model parameters for the exchange of Na^+ and H^+ on Dowex50-X8 resin behaved in a manner predictable from the theoretical derivation. In the case of upflow operation, the flow pattern agreed well with the modeling as one CSTR and one PFR in series.

Lucas *et al.* (1997) studied batch dynamics for the uptake of potassium from crude polyols on Amberlite 252, a strong acid ion exchange resin, results were obtained over a wide range of conditions. Experimental data have been analyzed using a homogeneous model with a finite solution volume. An increase of diffusion coefficients with the resin weight used in the purification was observed. An asymptotic maximum value, approaching the value of the diffusion coefficient in bulk solution, was reached for high resin weights or low values of external concentration. The heterogeneous nature of the resin matrix and the large size of the diffusing molecule were proposed as an explanation of this behavior. The proposed purification procedure finds general applicability for other polyol types, being economically and technically feasible.

2.2 Theory

2.2.1 Classification

Ion exchange resins can be classified into four main types: strongly acidic cation resin, strongly basic anion resin, weakly acidic cation resin, and weakly basic anion resin, all of which are dependent on the functional groups of the resins. Examples of resins and their properties are shown in Table 2.1.

Table 2.1 Types and properties of some resins.

Resin type	Structure	Functional group	pH range	Thermal stability (°C)
Strong acid	Gel	$—SO_3^-$	0-14	120
	Macroporous	$—SO_3^-$	0-14	120
Weak acid	Gel	$—COO^-$	4-14	120
	Macroporous	$—COO^-$	4-14	120
Strong Base (type1)	Gel	$—N(CH_3)_3^+$	0-14	80(Cl)
	Macroporous		0-14	40(OH)
Strong Base (type2)	Gel	$—N(CH_3)_2(CH_2CH_2OH)$	0-14	60(Cl)
	Macroporous		0-14	40(OH)
Weak Base	Gel	$—N(CH_3)_2$	0-9	100
	Macroporous		0-9	100
	Gel	polyamine	0-9	100

2.2.2 Mechanisms

Studies of ion exchange reactions on organic exchangers have identified the possible rate controlling steps, as shown in Figure 2.1, to be:

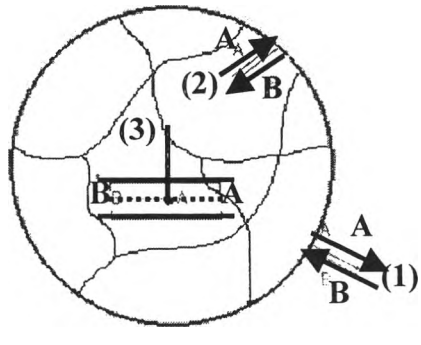

Figure 2.1 Rate determining steps in ion exchange.

1. Coupled diffusion or transport of counter-ions in the "external" solution phase.
2. Coupled diffusion or transport of counter-ions within the ion exchange resin.
3. Chemical reaction at the sites of the functional groups within the exchanger.

1. Coupled Diffusion of Counter-Ions in the"External" Solution

Rate control by mass transfer in the "external" solution is interpreted as *coupled mass transfer* across the hypothetical film or *Nernst layer* surrounding the resin particles by a mechanism of diffusion called *film diffusion.*

The driving force for mass transfer is the concentration difference or the concentration gradient of counter-ions between the two boundaries of the film. If theoretical refinements are ignored for the time being, the momentary flux equation for ion A may be written in terms of Fick's first law:

$$J_A = \frac{D_A \Delta C_A}{\delta} \qquad (2.1)$$

where C_A is the resin phase concentration of the counter-ion A initially in the exchanger, J_A is the flux (kmol m^{-2} s^{-1}) of ion A under a finite concentration difference ΔC_A (kmol m^{-3}) across the film of thickness δ (m).

2. Coupled Diffusion of Counter-ions in the Resin

Mass transfer in the film and resin particle are sequential processes and either process may be rate controlling. By a *simplified* analogy with the previous case for film diffusion, the average flux condition for transfer of ion A in the resin phase may be written:

$$\overline{J_A} = \frac{\overline{D}\Delta C_A}{r_0} \qquad (2.2)$$

Now, the driving force is the concentration gradient between the interior of the resin and the resin solution interface for ion A and resin beads of radius r_0. The bar notation represents the resin phase and $\overline{D}$ is an average diffusion coefficient for ions A and B within the resin. Resin phase diffusion coefficients are about one or two orders of magnitude smaller than found for aqueous solutions because of the steric resistance, The hindrance effect of the heterogeneous in resin structure on the ions diffused to the inside of resin, offered by copolymer matrix.

3. Chemical Reaction Rate Control

The true chemical reaction at the sites of the functional groups is represented purely schematically in Figure 2.1 by an imaginary transition state complex between ions A, B, and the inorganic group. Such a concept involves the making and breaking of ionic, covalent, or dative bonds, which has never been shown unequivocally to be solely rate controlling for the exchange of simple aqueous ions on organic exchangers. Reactions between simple, freely dissociated, aqueous ions are usually very fast and therefore not rate controlling, but some published data suggest chemical reaction rate

control for the exchange of transition metal ions or complex ions capable of strong chelate, which occur by following the chelating step, the co-ordination complex formation between the heavy metals and electron pair donating ligands, type complex formation with iminodiacetate or phosphonate functional groups.

2.2.3 Selectivity / Affinity

Relative affinity is one of the other quantities that is used to explain what type of cations and anions are convenient for resinous exchangers. The following sequences represent the order usually found for dilute solutions of commonly encountered ions with standard resins ($A^+ > B^+$: the ion A has the selectivity value for each type of resin higher than that of ion B).

Strong Acid Cation Resin (styrenic-sulfonate):

$Ag^+ > Cs^+ > K^+ > NH_4^+ > Na^+ > H^+ > Li^+$; $Ba_2^+ > Pb_2^+ > Ag^+ > Sr_2^+ > Ca_2^+ > Ni_2^+ > Cd_2^+ > Cu_2^+ > Co_2^+ > Zn_2^+ > Mg_2^+ > Cs^+$

Weak Acid Cation (acrylic-carboxylate):

$H^+ >> Cu_2^+ > Pb_2^+ > Ni_2^+ > Co_2^+ > Fe_3^+ > Ca_2^+ > Mg_2^+ > Na^+ > K^+ > Cs^+$

Strong Base Anion –Type 1 (styrenic-quaternary ammonia):

$SO_4^{2-} > HSO_4^- > I^- > NO_3^- > Br^- > Cl^- > HCO_3^- > HSiO_3^- > F^- > OH^-$; $SO_4^{2-} > ClO_4^- > ClO^- > NO_3^-$

Strong Base Anion –Type 2 (styrenic - quaternary ammonium):

The slightly lower base strength of Type 2 strong base anion exchangers results in the relative affinity of hydroxide ion usual lying between that of fluoride ion and hydrogencarbonate ion.

Weak Base Anion (styrenic – amine):

$$OH^- >> SO_4^{2-} > HSO_4^- > I^- > NO_3^- > Br^- > Cl^- > F^-$$

Generally: for all cation and anion exchange affinities on resins,

$$ION^{|z+1|} > ION^{|z|}$$

where z is the electrovalency of the ion (±).

2.3 Theoretical Consideration of Ion-Exchange Kinetics

The ion-exchange operation can be divided into three main modes: batch, fixed-bed and fluidized-bed operation. Each of these modes of operation and its theory is described below.

2.3.1 Batch Operation

In batch operation, the whole of the electrolyte solution is contacted with the ion-exchange resin particles. Therefore, the aqueous phase is homogeneous. This application is the simplest mode but its efficiency is limited by the selectivity of the resin under equilibrium. Manantapong (1997) studied the exchange of sodium ions in solution with hydrogen ions in the resin phase, and the process was represented by the exchange equation (2.3).

$$RSO_3H + NaCl \leftrightarrow RSO_3Na + HCl \quad (2.3)$$

RSO_3H and RSO_3Na are in the resin phase and NaCl and HCl are in the solution phase. From Manantapong's work, it was shown that the adsorption equilibrium was reached faster when a higher mixing rate was applied. It also revealed that increasing the initial concentration resulted in an increase of the solution uptake in the resin phase. For the exchange of calcium ions in solution with hydrogen ions in the resin phase, the process was represented by the exchange equation (2.4).

$$RSO_3H + CaCl_2 \leftrightarrow RSO_3Ca + 2HCl \quad (2.4)$$

RSO_3H and RSO_3Ca are in the resin phase and $CaCl_2$ and HCl are in the solution phase.

Simple material balances for ions can be written as

Mole of Ca^{2+} going to resin = Mole of H^+ going to solution

$$2V_R q = V_L h \quad (2.5)$$

Mole of Ca^{2+} before adsorption = Mole of Ca^{2+} after adsorption

= Mole of Ca^{2+} adsorbed onto the resin + Mole of Ca^{2+} in the solution (not adsorbed by resin)

$$2V_L c_0 = 2V_R q + 2V_L c \qquad (2.6)$$

where

V_R = volume occupied by the resin bed

V_L = volume occupied by the liquid bed

c_0 = initial concentration of calcium chloride

h = concentration of hydrogen ion in the solution phase

q = concentration of calcium ion in the resin

c = concentration of calcium ion in the solution phase

eq = amount of ion divided by its ion charge named equivalent

$eq = \frac{\text{molar mass}}{\text{ion charge}} = \frac{\text{mole of ion .}}{\text{ion charge}}$

In the batch part, a series of batch adsorption experiments was carried out in order to develop a relationship between the concentration of metal ions on the resin and in the solution at equilibrium (q^e and c^e) and an expression for the rate of adsorption (see section 4.2 in results and discussion part).

2.3.2 Fluidized-Bed Operation (Upflow Direction)

For upflow operation, the bed of solid particles was lifted and agitated by increasing the flow rate of fluid. When increasing the flow rate, particles move apart and the bed starts to expand. The void fraction of the bed can be calculated for any known height, H, from:

$$H = H_0\left(\frac{1-\varepsilon_0}{1-\varepsilon}\right) \qquad (2.7)$$

where

H = height of fluidized bed

H_0 = height of compacted bed

ε_0 = compacted bed void fraction, 0.41

ε = bed void fraction.

Manantapong (1997) and Tresattayawed (1999) studied the behavior of the fluidized bed operation of Na^+/H^+ and $Ca^{2+}/Mg^{2+}/H^+$, respectively. The previous researchers developed a model to predict the rate of metal ions adsorbed on the resin. The rate of adsorption is shown in equation (2.8):

$$r = \frac{dq}{dt} = k_1\left[\frac{q_t}{1+\frac{h}{k_2 c}} - q\right] \qquad (2.8)$$

where

q = concentration of NaCl, $CaCl_2$ or $MgCl_2$ in the resin phase

q_t = total exchange capacity of the resin

c = concentration of NaCl, $CaCl_2$ or $MgCl_2$ in the solution phase

h = hydrogen concentration in the solution phase.

2.3.3 Fixed-Bed Operation (Downflow Direction)

For downflow operation, the solution is passed through the resin bed in the downward direction. The uppermost portion of the column constantly contacts fresh electrolyte whereas the lower portions contact the electrolyte not adsorbed by the upper exchange. This procedure permits the resin bed to become fully exhausted, first at the top and then gradually downwards.

2.4 Description of Process Kinetic Models

The mechanism of ion exchange was expressed by the governing equations, which can been solved analytically or numerically. The solution is valid if it is compatible with the experimental data. The assumptions made in the derived equation are:

1. The resin particles are uniform.
2. Equilibrium exists at the liquid-solid interface.
3. There are no gradients in the resin, so the concentration in the resin is uniform.
4. The driving force involve in the mass transfer is expressible in terms of concentrations, and chloride ions in the solution do not affect the process.
5. The influence of counter-diffusion of the exchange ion from the resin of the solution is neglected.

2.4.1 Modeling the Response Time of pH Electrode

The hydrogen ions at the exit of the column were measured by a pH electrode, which did not provide an instantaneous measurement, because there is some lag, called the *response time*, of the electrode to detect the pH value of the solution. The model to account for the response time can be developed by examining Figure 2.2.

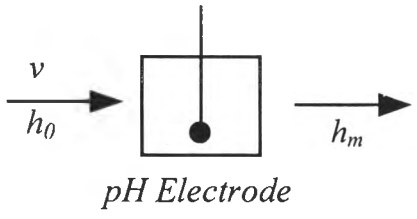

Figure 2.2 Representation of the response time experiment.

The governing equation for the response time is

$$\frac{dh_m}{dt} = \alpha_e (h_0 - h_m) \qquad (2.9)$$

where

h_0 = entering H^+ concentration

h_m = H^+ concentration measured by the pH electrode

α_e = response time constant of the pH electrode.

2.4.2 Modeling No Adsorption with Downflow Operation

The theory developed here was applied to the ion-exchange column performed under downflow or fixed-bed operation. The non-ideal PFR, consisting of one CSTR and one ideal PFR connected in series, was applied for the flow whose characteristic description is shown in Figure 2.3.

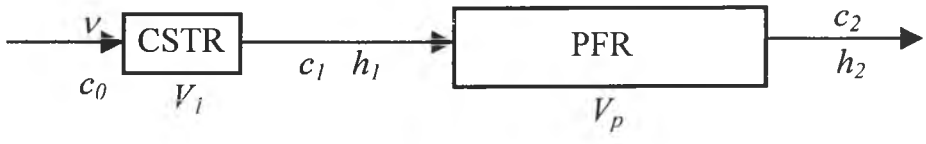

Figure 2.3 Representation of no adsorption experiment as one CSTR and one ideal PFR in series.

Theory

The H^+ balance on the CSTR was described by:

$$\frac{dh_1}{dt} = \frac{\upsilon}{V_1}(h_0 - h_1) \qquad (2.10)$$

where

h_0 = initial hydrogen ion concentration

h_1 = hydrogen ion concentration at the exit of CSTR

ν = volumetric flow rate of solution

V_1 = volume of CSTR.

The effect of a plug flow reactor for fixed-bed (downflow) operation can be described by using the *method of characteristics for hyperbolic equations* together with a completely *implicit approach* for finding the Ca^{2+} concentration on the resin and in the solution, q, c, at any time and length along the column.

Mathematical modeling for the no adsorption test was developed first and then used in the adsorption kinetics part. By setting the rate of adsorption equal to zero and fitting the experimental data with the model, the volume of the CSTR can be determined (the results are shown in Appendix B).

2.4.3 Modeling Adsorption with Downflow Operation

The mathematical model developed from the *no-adsorption test* was used in this part with the incorporation of the rate of adsorption as defined by equation (2.12). The theoretical results can be compared with the experimental data after including the small volume of a CSTR into the model (the results are shown in Appendix C). Also, the non-ideal PFR, consisting of one CSTR and one ideal PFR connected in series, was applied for flow characteristic flow description, as shown in Figure 2.4.

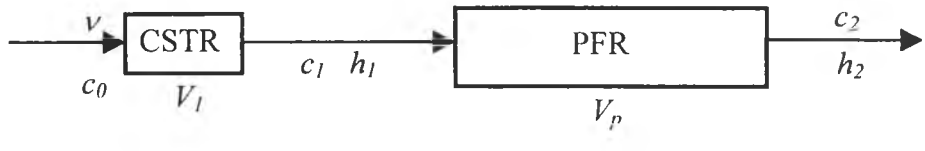

Figure 2.4 Representation of ion-exchange column as one CSTR and one ideal PFR in series.

Theory

Ca^{2+} balance on the CSTR (without reaction)

$$\frac{dh_1}{dt} = \frac{\upsilon}{V_1}(h_0 - h_1) \qquad (2.11)$$

The rate of calcium uptake by resin can be expressed by using the batch adsorption results

$$r = \frac{dq}{dt} = K(q^e - q) \qquad (2.12)$$

where

$$q^e = \beta(C^e)^{1/n} \qquad (2.13)$$

in which

c_0	=	initial calcium concentration
c_1	=	Ca^{2+} concentration at the exit of CSTR
c^e	=	Ca^{2+} concentration in the solution at equilibrium
ν	=	superficial velocity
V_R	=	volume occupied by the resin bed in the column
V_L	=	volume occupied by the liquid bed in the column
q	=	Ca^{2+} concentration onto the resin
q^e	=	Ca^{2+} concentration onto the resin at equilibrium
K	=	rate constant
β	=	constant, ν*dt/V_1
n	=	constant.

2.5 Method of Characteristics for Solving the Hyperbolic System of Equations for the Ion-Exchange Column

Due to the adsorption in the fixed-bed operation, in the downflow direction, the concentrations of ions in the liquid and on the resin depend upon both distance along the column, x, and time, t, so the *method of characteristics for hyperbolic equations* is necessary for solving this problem.

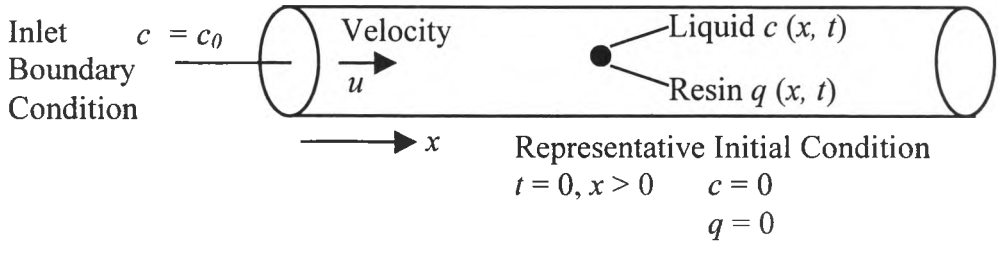

Figure 2.5 Representation of ion-exchange column in fixed-bed operation.

Ion Balance on Liquid

$$u\frac{\partial c}{\partial x} + \varepsilon\frac{\partial c}{\partial t} = -r \qquad (2.14)$$

Ion Balance on Resin

$$(1-\varepsilon)\frac{\partial q}{\partial t} = r \qquad (2.15)$$

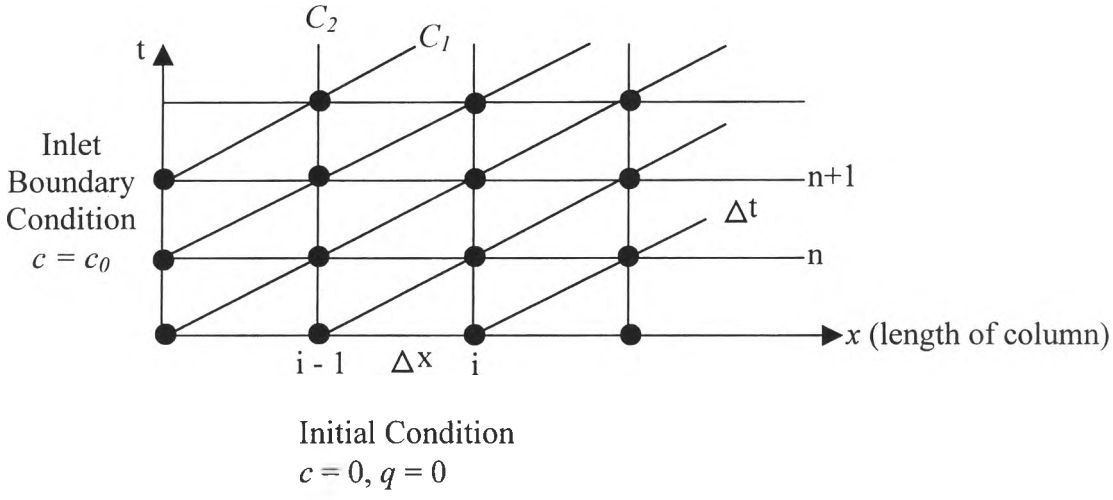

Figure 2.6 A diagram of grid points together with C_1 and C_2 direction.

Characteristic directions

C_1 direction: relates to an observer travelling with the liquid

C_2 direction: relates to an observer on a fixed resin particle

$$C_1 \qquad \frac{dx}{dt} = \frac{u}{c} \qquad\qquad C_2 \qquad \frac{dx}{dt} = 0$$

The partial differential equations can be written

Along C_1:

$$\frac{dc}{dt} = \frac{\partial c}{\partial t} + \frac{\partial c}{\partial x}\frac{dx}{dt} \qquad (2.16)$$

$$= \frac{1}{\varepsilon}\left(\varepsilon\frac{\partial c}{\partial t} + u\frac{\partial c}{\partial x}\right) = -\frac{r}{\varepsilon}$$

Along C_2:

$$\frac{dq}{dt} = \frac{\partial q}{\partial t} + \frac{\partial q}{\partial x}\frac{dx}{dt} = \frac{r}{1-\varepsilon} \qquad (2.17)$$

The equations shown below can be used together with a completely *implicit approach* for finding the Ca^{2+} concentration on the resin, q, and in the solution, c at any time and length along the column. Finally, the theoretical values of q and c at the exit of the column are compared with the experimental data.

$$C_1: \quad \frac{dc}{dt} = \frac{-r}{\varepsilon} \quad along \quad \frac{dx}{dt} = \frac{u}{\varepsilon} \qquad (2.18)$$

$$C_2: \quad \frac{dq}{dt} = \frac{r}{1-\varepsilon} \quad along \quad \frac{dx}{dt} = 0 \qquad (2.19)$$

where r was given by equation (2.12)

2.6 Completely Implicit Approach

Fortunately, the above system of ordinary differential equations can be solved by using a *conventional finite-difference* method. Equations (2.20) and (2.21) give a completely *implicit approach* for finding the Ca^{2+} concentration on the resin, q, and in the solution, c at any time and length along the column.

Finally, the theoretical values of q and c at the exit of the column can be compared with the experimental data. This method involves two unknowns, at time $t + dt$, which can be obtained from two equations by using the iteration method as discussed in Appendix G to find the final (real) answer. The two finite-difference equations have the values of both c and q at time $t + dt$. The equations used to predict the value of q and c at time $t + dt$ are

Along the C_1 direction, equation (2.16) becomes

$$\frac{c_{i,n+1} - c_{i-1,n}}{\Delta t} = \frac{-r}{\varepsilon} = \frac{-K}{\varepsilon}\left(\beta c_{i,n+1}^{1/n} - q_{i,n+1}\right) \qquad (2.20)$$

Along the C_2 direction, equation (2.17) becomes

$$\frac{q_{i,n+1} - q_{i,n}}{\Delta t} = \frac{r}{1-\varepsilon} = \frac{K}{1-\varepsilon}\left(\beta c_{i,n+1}^{1/n} - q_{i,n+1}\right) \qquad (2.21)$$

where

c	=	Ca^{2+} concentration in the solution
c_0	=	initial calcium concentration
$c_{i,n}$	=	Ca^{2+} concentration in the solution at time i and distance subscript n
$c_{i,n+1}$	=	Ca^{2+} concentration in the solution at time i and distance subscript n+1
u	=	superficial velocity
x	=	length of column
q	=	Ca^{2+} concentration onto the resin
$q_{i,n}$	=	Ca^{2+} concentration onto the resin at time i and

distance subscript n

$q_{i,\,n+1}$ = Ca^{2+} concentration onto the resin at time i and distance subscript n+1

dq/dt = adsorption rate

dc/dt = desorption rate

K = rate constant

ε = void fraction of resin

β = constant, $v^{*}dt/V_1$

n = constant.